© 2017. Published by The Company of Biologists Ltd | Journal of Experimental Biology (2017) 220, 4743-4744 doi:10.1242/jeb.173849

CORRECTION

Correction: The energetic cost of filtration by demosponges and their behavioural response to ambient currents

Danielle A. Ludeman, Matthew A. Reidenbach and Sally P. Leys

There was an error published in *J. Exp. Biol.* **220**, 995-1007.

Some values for head loss and respiration in Table 3 were carried over from an earlier version of the manuscript. The corrected table follows.

The final numbers for volume flow rate, head loss, pumping power and cost of pumping remain unchanged, and there are no changes to the results and conclusions of the paper. The data available from the University of Alberta Education Resource Archive (ERA; https://doi.org/10.7939/R36688W8N) are correct. The authors apologise for any inconvenience this may have caused.

Journal of Experimental Biology

Table 3. Morphometric model of the aquiferous system in five species of demosponges

Region of the aquiferous canal system	*Neopetrosia problematica*				*Haliclona mollis*				*Tethya californiana*				*Callyspongia vaginalis*				*Cliona delitrix*			
			H (μm H_2O)				*H* (μm H_2O)				*H* (μm H_2O)				*H* (μm H_2O)				*H* (μm H_2O)	
	A_i (mm^2)	u_i (mm s^{-1})	Riisgård and Larson (1995)	Leys et al. (2011)	A_i (mm^2)	u_i (mm s^{-1})	Riisgård and Larson (1995)	Leys et al. (2011)	A_i (mm^2)	u_i (mm s^{-1})	Riisgård and Larson (1995)	Leys et al. (2011)	A_i (mm^2)	u_i (mm s^{-1})	Riisgård and Larson (1995)	Leys et al. (2011)	A_i (mm^2)	u_i (mm s^{-1})	Riisgård and Larson (1995)	Leys et al. (2011)
Ostia	3.37	1.04	111	4	0.90	3.90	709	42	1.38	1.76	113	2	12.8	0.68	51	1	2.82	6.57	409	9
Subdermal space	19.7	0.18	10	1	22.2	0.16	10	96	16.7	0.14	4	2	21.8	0.40	6	7				
Large incurrent canal	15.9	0.22	19	19	14.4	0.24	9	6	21.7	0.11	1	1	14.1	0.62	14	14	3.31	5.60	288	288
Medium incurrent canal	7.21	0.49	57	57	3.21	1.09	204	45	24.8	0.10	17	17	2.70	3.25	244	244	2.57	7.22	1322	1322
Small incurrent canal	5.79	0.61	612	612	4.16	0.84	215	278	3.66	0.66	166	166	3.67	2.39	2	2	1.71	10.84	2956	2956
Prosopyles	494	0.007	5	1	346	0.010	11	330	172	0.014	8	2	55.2	0.159	228	120	17.7	1.04	937	307
Pre-collar space	255	0.014	95	95	775	0.005	2	5	504	0.005	19	19	170	0.051	2195	2195	264	0.070	1288	1288
Collar slit	**376**	**0.009**	**288**	**541**	**546**	**0.006**	**471**	**73**	**1237**	**0.0020**	**147**	**212**	**492**	**0.018**	**668**	**2839**	**1095**	**0.017**	**2300**	**474**
Post-collar space	412	0.009	12	12	405	0.009	12	9	1077	0.0022	7	7	566	0.015	15	15	1019	0.018	40	40
Chamber	408	0.009	2	2	171	0.020	3	1	488	0.005	1	1	406	0.022	4	4	674	0.027	7	7
Apopyle	208	0.02	3	0	44.6	0.08	14	0	110	0.02	63	60	40.3	0.22	85	12	52.1	0.36	195	39
Small excurrent canal	4.66	0.75	282	282	6.79	0.52	160	24	2.47	0.98	264	264	0.52	16.9	12	12	1.71	10.84	2956	2956
Medium excurrent canal	3.47	1.01	172	172	6.33	0.55	56	52	24.8	0.10	15	15	2.87	3.05	411	411	2.57	7.22	1322	1322
Large excurrent canal	1.21	2.90	471	471	13.1	0.27	6	13	21.7	0.11	1	1	3.04	2.88	132	132	3.31	5.60	288	288
Osculum	0.26	13.66	0	33	0.12	30.44	0	33	0.11	21.95	0	3	0.15	59.33	0	176	0.17	110.41	1	8
Volume flow rate, Q (ml min^{-1})			9.0				48.6				82.1				742				2668	
Respiration, R_{tot} (μW)			87				807				1426				14,218				42,102	
Head loss, ΔH (μm H_2O)			2138	2303			1881	1008			826	771			4066	6185			14,307	11,304
Pumping power, P_p (μW)			3	3			15	8			11	11			504	766			6377	5038
Cost of pumping, η (%)			3.70	3.99			1.89	1.01			0.80	0.74			3.54	5.38			15.15	11.97

A_i is the estimated total cross-sectional area for each region from the dimensions listed in Table 2. The velocity of water flow through each area u_i was calculated from cross-sectional area A_i and measured excurrent velocity u_{ex} out of the osculum using Eqn 1. Head loss H in each region was calculated using Eqns A1–A5 from dimensions and velocity u_i of each region. Riisgård and Larson's (1995) model used a different equation of head loss for each region of the aquiferous canal system, whereas Leys et al.'s (2011) model used only Eqn A2. The sum of the head loss ΔH and measured volume flow rate are used to calculate the pumping power P_p using Eqn A6. The cost of pumping η (%) is then estimated using Eqn A7 from the pumping power P_p and the measured respiration rate R_{tot}. The collar slit is in bold, representing the filtration apparatus.

Journal of Experimental Biology (2017) 220, 4743-4744 doi:10.1242/jeb.173849

© 2017. Published by The Company of Biologists Ltd | Journal of Experimental Biology (2017) 220, 995-1007 doi:10.1242/jeb.146076

RESEARCH ARTICLE

The energetic cost of filtration by demosponges and their behavioural response to ambient currents

Danielle A. Ludeman[1], Matthew A. Reidenbach[2] and Sally P. Leys[1,*]

ABSTRACT

Sponges (Porifera) are abundant in most marine and freshwater ecosystems, and as suspension feeders they play a crucial role in filtering the water column. Their active pumping enables them to filter up to 900 times their body volume of water per hour, recycling nutrients and coupling a pelagic food supply with benthic communities. Despite the ecological importance of sponge filter feeding, little is known about how sponges control the water flow through their canal system or how much energy it costs to filter the water. Sponges have long been considered textbook examples of animals that use current-induced flow. We provide evidence that suggests that some species of demosponge do not use current-induced flow; rather, they respond behaviourally to increased ambient currents by reducing the volume of water filtered. Using a morphometric model of the canal system, we also show that filter feeding may be more energetically costly than previously thought. Measurements of volumetric flow rates and oxygen removal in five species of demosponge show that pumping rates are variable within and between species, with the more oxygen consumed the greater the volume filtered. Together, these data suggest that sponges have active control over the volume of water they process, which may be an adaptation to reduce the energetic cost of filtration in times of high stress.

KEY WORDS: Porifera, Filter feeding, Passive flow, Current-induced flow, Oxygen, Energetic cost

INTRODUCTION

Benthic suspension feeders affect marine and freshwater ecosystems by ingesting suspended particulates and dissolved nutrients from the overlying water column and releasing by-products for use by other organisms (Gili and Coma, 1998). Recycling of nutrients in this way provides an important link between the benthic and pelagic communities, known as benthic–pelagic coupling, yet the energetic cost of this type of feeding in invertebrates is still debated. Some work suggests the cost of pumping for filtration is minimal (Riisgård and Larsen, 1995, 2001), while other studies estimate that filtration can make up a quarter of the costs of metabolism (e.g. Hadas et al., 2008).

Many suspension feeders use ciliary or muscular pumps to induce water currents that draw water with food towards themselves. Bivalves, ascidians, polychaetes and sponges use filters to strain out particles from the water that are too small to be captured individually (Jørgensen, 1966). Where suspended particulates are low in concentration, this approach can be highly efficient to process large volumes of water (Jørgensen, 1966), and so it has been suggested that filter feeders evolved a low energetic cost of filtration to allow continuous feeding (Jørgensen, 1975). Yet, food availability varies widely on a temporal basis, with fluctuations occurring seasonally, daily and with the ebb and flood of the tide. It would therefore be advantageous for filter feeders to sense the variations in food availability and feed when concentrations are high. Two examples suggest this behaviour does occur. Bivalves respond to food availability by reducing filtration and respiration rates when food is scarce (Thompson and Bayne, 1972; Griffiths and King, 1979), and the demosponge *Tethya crypta* reduces pumping activity at night when ambient currents are lower (Reiswig, 1971); lower ambient currents often correspond with reduced food availability (Newell and Branch, 1980). As all filter feeders demonstrate some fluctuations in pumping rates in response to variations in environmental cues, filtration may be more costly than previously thought and the animals may be finely adapted to habitats that support the energetic cost to obtain food.

Models of the filter and pump system for a number of invertebrates have suggested that filter feeding is inexpensive, at less than 4% of total metabolism (Riisgård and Larsen, 1995). In contrast, direct measurements of the uptake of oxygen going from non-feeding to feeding has shown that in bivalves filtration accounts for up to 50% of total metabolism (Thompson and Bayne, 1972; Newell and Branch, 1980) and in sponges 25% of total respiration (Hadas et al., 2008). In addition, the resistance through the filter of sponges may be much higher than previously thought owing to the narrow dimensions of a difficult-to-preserve fine mucus mesh on the collar filter (Leys et al., 2011).

In support of the theory that the cost of filtration may be high, some animals have been found to reduce the energy expended by using ambient currents to draw water through the filter, for example, by dynamic pressure, the Bernoulli effect or viscous entrainment. In high-current environments, barnacles switch from active to passive feeding and orient their bodies toward the current (Trager et al., 1990). Cnidarians (Best, 1988), ascidians (Young and Braithwaite, 1980; Knott et al., 2004) and brachiopods (LaBarbera, 1977) also orient their bodies to the current, while other invertebrates may take advantage of current-induced flow through tubes (Vogel, 1977; Murdock and Vogel, 1978; von Dassow, 2005; Shiino, 2010). Sponges are often considered textbook examples of the use of current-induced flow in nature (Bidder, 1923; Vogel, 1974, 1977) but experiments to confirm this have been equivocal (Leys et al., 2011).

Even if models are correct and the cost of filtration is not great, a universal cost for all sponges is unlikely because structural differences in the sponge canal system owing to body form (Reiswig, 1975a), microbial content (Weisz et al., 2008) and tissue

[1]Department of Biological Sciences, University of Alberta, CW 405 Biological Sciences Building, Edmonton, Alberta T6G 2E9, Canada. [2]Department of Environmental Sciences, University of Virginia, 291 McCormick Rd, Clark Hall, Charlottesville, VA 22904, USA.

*Author for correspondence (sleys@ualberta.ca)

S.P.L., 0000-0001-9268-2181

Received 13 July 2016; Accepted 20 December 2016

Journal of Experimental Biology (2017) 220, 995-1007 doi:10.1242/jeb.146076

density (Turon et al., 1997) can cause wide differences in filtration rates between species. Temperature and food availability vary across habitats, causing differences in seawater viscosity and enzyme function that potentially lead to differences in the metabolic cost of filtering in different habitats. Estimates of the cost of pumping for a range of sponge species and habitats are therefore required to better understand sponge energy budgets.

Models can be informative about which structures contribute most to energetic costs; however, their accuracy depends on having correct dimensions for each region of the filter and canal system as well as volumetric flow rates. This approach used by Riisgård et al. (1993) was recently used for the filtration system of the glass sponge *Aphrocallistes vastus* (Leys et al., 2011), where the cost of pumping was found to be 28% of the total metabolism. Here, the resistance through the filter was found to be much higher than previous estimates for demosponges because of the small spaces of the glycocalyx mesh (Leys et al., 2011), a structure that is often not preserved with common fixation techniques and was not included in the model used by Riisgård et al. (1993). In addition, the volumetric flow rate in *A. vastus* was quite high compared with the 'standard sponge' studied by Riisgård et al. (1993), where volumetric flow rate was obtained indirectly using clearance rates of particles (flagellate cells) during incubation in a closed vessel. Closed vessels have been shown to cause reduced pumping behaviour of sponges (Yahel et al., 2005; Hadas et al., 2008), and the sponge may re-filter the water if sampling times are not well adjusted to pumping rates (Yahel et al., 2005). In contrast, Leys et al. (2011) used direct sampling of incurrent and excurrent water to determine filtration and pumping rates *in situ*.

To evaluate the importance of accurate measures of filter dimensions and volume of water processed when estimating the cost of filtration, we first examined the effect of changes in these values calculated in previous work. We then studied energetics of filtration in five species of demosponge from tropical and temperate habitats using *in situ* measurements of oxygen consumption and pumping rate, experimental tests of pumping at different ambient flow rates, and morphometric analysis of the canal and filter structures.

MATERIALS AND METHODS

Meta-analysis

We first carried out a meta-analysis using data from the literature to determine the cost of pumping in four filter-feeding invertebrate groups used by Riisgård and Larsen (1995). Dimensions were calculated from electron micrographs of mucus filters (Fig. S1), where available, and volume flow rates that were obtained using 'direct' methods were used.

Field and laboratory studies

Field work was carried out at the Bamfield Marine Sciences Centre (BMSC) in Bamfield, British Columbia, Canada, and the Smithsonian Tropical Research Institute (STRI) on Isla Colon in Bocas del Toro, Panama. At BMSC, three species of demosponge, *Neopetrosia problematica* (n=7), *Haliclona mollis* (n=10) and *Tethya californiana* (n=8), were collected by SCUBA from Barkley Sound and kept in seawater tables at 8–9°C with unfiltered water from 30 m depth at flow rates of 3000 l min^{-1}.

Measurements on *Cliona delitrix* (n=8) and *Callyspongia vaginalis* (n=11) were conducted *in situ* by snorkeling at STRI Point (9°21.169′N, 82°15.528′W; Diaz, 2005), at approximately 2 m depth where seawater was 28–29°C. An aluminum frame (80/20 Inc., Columbia City, IN, USA) was placed over the sponge and instruments were attached using Loc-Line (Lockwood Products, OR, USA) and clamps (Fig. 1). The instruments were tethered via cables to a laptop computer on a boat anchored near the study site to monitor the data collection in real time.

Measurements of excurrent velocity

Excurrent velocity was measured using a Vectrino II profiling acoustic Doppler velocimeter (ADV, Nortek, Rud, Norway), which provided 30 velocity estimates in 1 mm vertical bins, within a sampling diameter of approximately 6 mm. Because the sampling volume is some distance from the probe head, and because the excurrent 'jet' from a sponge osculum may be small, and may not travel very far from the osculum lip, positioning it over the sponge osculum is challenging. Fluorescein dye diluted in 0.2 µm filtered seawater was used to visualize the excurrent flow (Fig. S2), and a plastic cable tie was used to indicate the specific position of the sampling volume by blocking the signal. However, the profiling capabilities of the Vectrino II also helps because the ADV takes measurements over the full 30 mm vertical profile, and as a result the lip of the sponge osculum itself disrupts the profile, showing exactly where the sampling volume is above the sponge (Fig. S2). Using this method, it is possible to be sure that the velocity being recorded is just inside the sponge osculum, and this becomes important in preventing interference with ambient water velocities. For the three temperate sponge species the sample volume diameter (6 mm) was greater than the diameter of the oscula and therefore the profiler

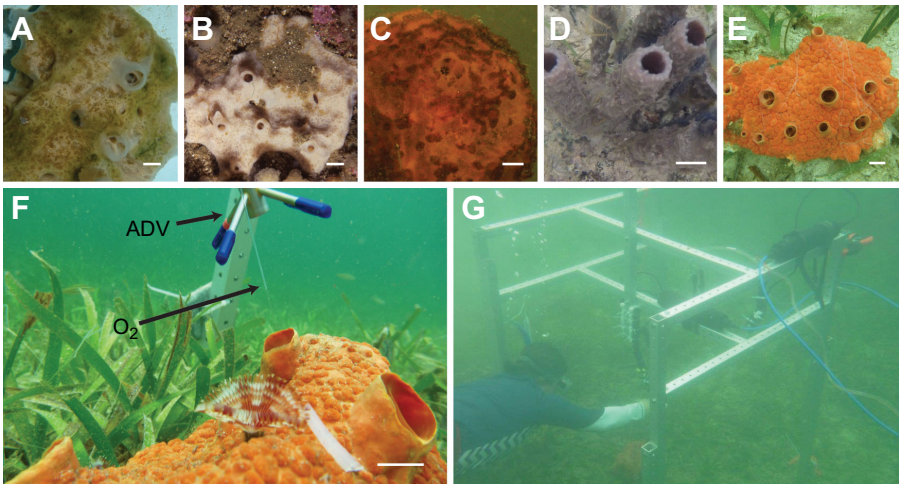

Fig. 1. Experimental setup and study species. *Haliclona mollis* (A), *Neopetrosia problematica* (B) and *Tethya californiana* (C) were collected and studied *in vitro* in Bamfield, British Columbia, Canada. *Callyspongia vaginalis* (D) and *Cliona delitrix* (E) were studied *in situ* in Bocas del Toro, Panama. (F) Excurrent velocity was measured out of the osculum using a Nortek Vectrino II acoustic Doppler velocity (ADV) and removal of oxygen was measured using a FirestingO_2 bare fibre sensor (O_2) positioned inside the sponge osculum. (G) Instruments were mounted *in situ* on a frame positioned over the sponge. Scale bars: (A,C) 0.5 cm; (B) 1 cm; (D–F) 2 cm.

Journal of Experimental Biology

Journal of Experimental Biology (2017) 220, 995-1007 doi:10.1242/jeb.146076

captured the average velocity across the full osculum. However, for the two warm-water sponges, the sampling volume was smaller than the osculum diameter. Because we sampled just inside the osculum, and because ambient flow could be seen to affect scalar (x,y,z) velocity (Denny, 1993) (Table S1), we therefore only used the **Z** velocity vector as a conservative measure of the average excurrent velocity of each osculum.

The ADV sensor was attached to Loc-Line for fine positioning above the sponge osculum to obtain the position of maximum excurrent velocity. Once the sensor was oriented correctly, excurrent velocity was recorded for 5 min at 25 Hz on low power (high power was strong enough to push the excurrent flow down, a process termed streaming). Data were binned using a 5 s median filter in MATLAB (vR2013b; MathWorks, Natick, MA, USA). Images of each sponge osculum were taken using a GoPro Hero2 for the duration of the recording and their diameters were measured in ImageJ (v. 1.43r; National Institutes of Health, Bethesda, MD, USA) to calculate volumetric flow.

Sponge volumes and surface area for each of the species were calculated by measuring the dimensions of the sponge from images taken of whole animals *in situ*, and using ImageJ (v. 1.43r). Volumes and surface areas were estimated as a cylinder (*C. vaginalis*), an ellipsoid (*C. delitrix* and *H. mollis*) and a sphere (*T. californiana*). When there was more than one osculum per sponge, sponge volume was calculated and divided by the number of oscula to obtain sponge volume per osculum. Because *C. delitrix* bores into coral, the ratio of sponge to coral skeleton in *C. delitrix* was estimated by dissolving the coral skeleton using 5% ethylenediamenetetracetic acid (EDTA) for a piece approximately 2 cm^3, or 4.5 g, and scaling up to the whole specimen using the relative immersed volumes. *Neopetrosia problematica* is highly irregular in shape; therefore, a combination of triangles was used to estimate volume and surface area. The ratio of sponge volume to dry weight was calculated by drying three pieces of each species at 100°C to constant mass. This ratio was then used to standardize volume flow rate to dry weight.

Measurements of oxygen consumption

Ambient and excurrent oxygen were measured using a two-channel FireStingO_2 optical oxygen metre (Pyro Science, Germany) with 250 µm diameter bare fibre minisensor probes. Before positioning the excurrent sensor in the sponge osculum, both probes were left in ambient water for at least 5 min to determine the difference in readings between the two sensors (here termed the offset value); this difference was subtracted from the difference between ambient and excurrent oxygen for all analyses. Oxygen sensors were calibrated to 21% (saturated water) and zero oxygen prior to experiments using air-bubbled water and a solution of sodium hydrosulfite. Oxygen readings were corrected using both internal and external temperature probes directly by instrument and recorded in mg l^{-1}. In addition, the ambient and excurrent sensors were positioned at the same height in the water column, such that any temperature fluctuations were accounted for between probes. Data were collected every 1 s and binned using a 5 s median filter using MATLAB (vR2013b). Oxygen removal per hour was calculated using the volume of water filtered per hour, and standardized to per gram dry weight.

Effects of ambient current

To assess the effect of ambient current velocities on sponge excurrent flow, experiments were conducted on *C. delitrix* and *C. vaginalis* at STRI by manipulating ambient flow with an underwater aquarium pump (Eheim compact+3000). The pump was anchored near the sponges with a weight and the outflow was directed through a 50 cm long, 10 cm diameter PVC pipe at and over the sponges following the method of Genin et al. (1994). The aquarium pump had variable speeds that could generate flow at 5 to 40 cm s^{-1} through the PVC pipe when positioned 30 cm from the sponge, as measured in a flow flume. Three flow speeds were used in experiments by setting the pump to low, medium and high speeds. Ambient current velocity was recorded using a Vectrino I point ADV (Nortek) with a sampling volume of 6 mm by 7 mm, positioned approximately 10 cm from the sponge and perpendicular to the pump outflow (Fig. 1F). The ADV could not be positioned right next to the sponge because of interference between the ADVs. Data were measured with a transmit length of 1.8 mm at 25 Hz on high power and binned using a 5 s median filter using MATLAB (vR2013b).

Paired excurrent velocities and oxygen removal were measured during experiments as described above. The profiling ADV (Nortek) was first positioned to ensure maximum excurrent velocity recordings from the osculum. Then the oxygen sensor was positioned inside the osculum, ensuring that it did not interfere with the ADV sampling volume as determined by a probe check analysis. Paired recordings were measured for 5 min at each flow rate (no additional flow, low, medium and high pump setting), and this experiment was repeated three times.

A GoPro Hero2 camera with underwater dive housing was positioned on the frame above both sponges to record osculum size during the experiment; images were captured every 30 s and a ruler was positioned in one of the images for calibration. Changes in osculum area were measured using a script developed for MATLAB (vR2013b). Volume filtered was calculated using excurrent velocity and area of the osculum. The ratio of sponge volume to dry weight was used to standardize volume flow rate and oxygen removal to per gram dry weight.

Statistical analyses

All statistical analyses were completed using SigmaStat in SigmaPlot v12.5. Data were tested for normality and linearity and, subsequently, variables were tested for association using a Spearman's rank order correlation test to allow for non-linearity.

Morphometric analysis

For scanning electron microscopy (SEM), sponges were cut into 1 mm^3 pieces and fixed in a cocktail consisting of 1% OsO_4, 2% glutaraldehyde in 0.45 mol l^{-1} sodium acetate buffer with 10% sucrose at 4°C for 6–12 h (Harris and Shaw, 1984). Modifications included addition of 10% Ruthenium Red to some samples to preserve mucus on the collar filter and adding 4% OsO_4 directly to the sponge tissue before fixation as above, to minimize contraction of canals. Samples were rinsed in distilled water, dehydrated to 70% ethanol and desilicified in 4% hydrofluoric acid (HF) at room temperature (RT) to dissolve spicules. Following desilicification, samples were dehydrated through a graded series to 100% ethanol, fractured in liquid nitrogen and critical point dried. Pieces were mounted on aluminum stubs using an eyebrow brush, gold coated and viewed in a field emission scanning electron microscope (SEM; JEOL 6301 F). Some pieces of *C. delitrix* and *C. vaginalis* were embedded in paraffin wax, sectioned at 12 or 30 µm and mounted on aluminum stubs. Prior to embedding, *C. delitrix* (which bores into coral and so is surrounded by the coral skeleton) was placed in 5% EDTA for 24 h to remove the coral skeleton. After sectioning, the wax was removed in toluene for 15 min, and the stubs were gold coated and viewed in a field emission SEM.

Journal of Experimental Biology (2017) 220, 995-1007 doi:10.1242/jeb.146076

For histology, 1 cm^3 pieces of sponge were fixed in 4% paraformaldehyde in filtered seawater for 24 h, rinsed twice in phosphate buffered saline (PBS), dehydrated in 70% ethanol and desilicified in 4% HF/70% ethanol at RT for 24–72 h. *Cliona delitrix* was decalcified in Cal-Ex Decalcifier (Fisher Scientific) for 24 h. Tissue was embedded in paraffin wax and sectioned at 5 µm (*T. californiana*), 12 µm (*H. mollis* and *C. delitrix*) and 30 µm (*N. problematica* and *C. vaginalis*) and sections were stained in Masson's trichrome. Images were captured with a QiCam using Northern Eclipse v.7 (Empix Imaging Inc., Mississauga, ON, Canada) on a Zeiss Axioskop2 Plus microscope.

To determine resistance through the aquiferous system, dimensions of the canals and flagellated chambers were measured from both SEM and histological sections using ImageJ (v. 1.43r). Care was taken to select regions of the canal system that were not contracted by looking at the tissue surrounding the canal system. It was not always possible to identify incurrent versus excurrent canals; in these instances it was assumed that the dimensions and path length were the same between excurrent and incurrent canals, following Riisgård et al. (1993).

The cross-sectional area of each region of the aquiferous system was calculated for a 100 mm^3 (100 µl) piece after Reiswig (1975a) and Leys et al. (2011). Owing to differences in the shape of the sponge body, the dimensions for this 100 µl piece differed for each species. For *N. problematica*, *H. mollis*, *T. californiana* and *C. delitrix*, the inhalant surface was 4.5×4.5 mm and the wall 5 mm thick. The body wall of *C. vaginalis* was only 3 mm thick and therefore a larger inhalant surface was used (5.77×5.77 mm) to generate the same 100 µl volume for the piece.

Estimating resistance through the canal system

The cost of filtration can be estimated by the power needed to move water through the sponge aquiferous system. The power is estimated by converting oxygen used in filtration to watts of energy. The movement of water experiences friction from the small dimensions of the canal and filter system and this resistance is called the head loss. Therefore, to determine the cost of filtration, we calculated the velocity of water through each part of the sponges' aquiferous system, and then estimated the resistance (head loss) at each part of the aquiferous system.

The velocity of water through each region of the aquiferous canal system, u_i, was calculated using the estimated cross-sectional areas for each part of the sponge and known excurrent velocity from the osculum (Reiswig, 1975a):

$$u_i = \frac{u_{ex} A_{osc}}{A_i}, \quad (1)$$

where A_i is the cross-sectional area of the region, A_{osc} is the cross-sectional area of the osculum and u_{ex} is the measured excurrent velocity from the osculum.

Two separate approaches were used to estimate the resistance through the canal system of sponges. The first uses an approach summarized by Riisgård and Larsen (1995), where a different equation to model each region of the canal system is applied based on the characteristics of the region. The different equations in this first approach reflect the estimated different architectures of different regions of the sponge. The second approach uses only one equation for the whole canal system (Leys et al., 2011), based on the Hagen–Poiseuille equation for fully developed laminar flow in a tube. This approach assumes that different equations do not capture the accurate differences between regions and therefore one equation is more straightforward and just as accurate. A detailed description of the equations is provided in the Appendix.

RESULTS

Meta-analysis

Using both dimensions of filter size gathered from electron micrographs and direct volume flow rate measurements resulted in an increase in the estimate of the cost of filtration for taxa studied previously (polychaetes, sponges, tunicates), in some instances to more than five times previously calculated values (Table S2).

Volume flow rates and oxygen removal

Mean excurrent velocity, volumetric flow rate and oxygen removal for each species are provided in Table 1. *Cliona delitrix* had the fastest excurrent velocity; however, *C. vaginalis* had the highest volumetric flow rate (processed the most water) and used the most oxygen. *Tethya californiana* filtered the smallest volume of water per unit time and removed the least oxygen of all five species.

For all sponge species except *C. delitrix*, more oxygen was removed when more water was filtered (Fig. 2). For one individual of each species measured over a 5 min period, oxygen removal increased with volume filtered except for *C. delitrix* (*N. problematica*: r_S=0.813, P<0.0001; *H. mollis*: r_S=0.869, P<0.0001; *T. californiana*: r_S=0.905, P<0.0001; *C. delitrix*: r_S=−0.180, P=0.169; and *C. vaginalis*: r_S=0.734, P<0.0001; Fig. 2A). Mean oxygen removal between individuals of each species was also positively correlated with the amount of water filtered, again except for *C. delitrix* (r_S=0.843, P<0.0001; Fig. 2B).

Effect of ambient flow on pumping rates

Callyspongia vaginalis responded to changes in ambient flow with changes to both excurrent velocity and oxygen used, but the sponge's response depended on the magnitude of ambient current (Fig. 3A,B). An increase in ambient flow from 0 to 5 cm s^{-1} caused a reduction in both excurrent velocity and oxygen removal, but when ambient current rose from 5 to 15 cm s^{-1}, then excurrent velocity and oxygen removal both increased. At ambient currents greater than 15 cm s^{-1}, however, excurrent velocity and oxygen removal did not change

Table 1. Mean excurrent velocity, volume flow rate and oxygen removal from five species of demosponges

			Volume flow rate			Oxygen removal		
Species	*n*	Excurrent velocity (cm s^{-1})	l h^{-1}	l h^{-1} ml^{-1} sponge	l $h^{-1}g^{-1}$ DW sponge	µmol l^{-1}	µmol h^{-1} ml^{-1} sponge	µmol h^{-1} g^{-1} DW sponge
Cliona delitrix	8	11.04±0.54	175.04±38.83	0.39±0.02	4.33±0.21	2.20±1.04	0.83±0.38	9.32±4.29
Callyspongia vaginalis	10	5.93±0.67	44.49±7.29	1.13±0.18	18.02±2.95	2.63±0.53	3.12±0.99	49.72±15.87
Tethya californiana	9	1.95±0.30	5.16±0.73	0.09±0.007	0.28±0.02	2.71±0.60	0.23±0.04	0.71±0.12
Haliclona mollis	10	3.04±0.30	2.92±0.47	0.13±0.01	1.08±0.11	2.32±0.53	0.31±0.08	2.53±0.63
Neopetrosia problematica	6	1.37±0.25	0.53±0.11	0.28±0.05	2.26±0.41	1.35±0.14	0.38±0.07	3.08±0.63

Data are means±s.d. Both volume flow rate and oxygen removal are standardized by sponge volume (per ml sponge) and sponge weight [per gram dry weight (DW)].

Journal of Experimental Biology

Journal of Experimental Biology (2017) 220, 995-1007 doi:10.1242/jeb.146076

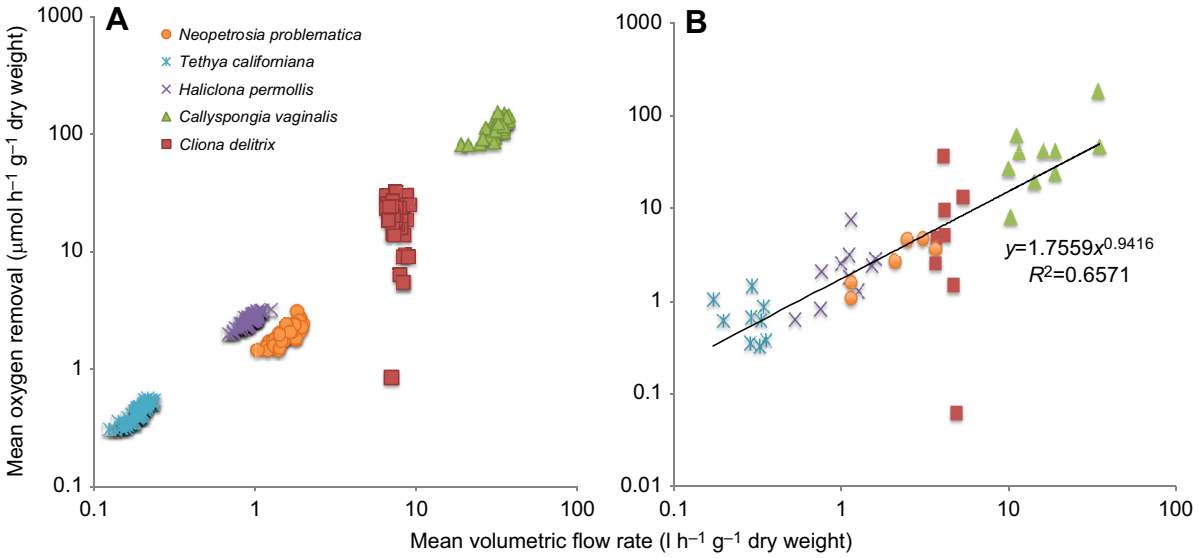

Fig. 2. Volumetric flow rates and oxygen removal. (A) Volumetric flow (l h^{-1} g^{-1} dry weight) and oxygen removal (µmol h^{-1} g^{-1} dry weight) were recorded for 5 min and plotted for one individual of each of five species of demosponges. Oxygen removal increased as the volume filtered increased across species, with the exception of *C. delitrix* (red). (B) The same trend is seen for oxygen removal and volumetric flow for multiple individuals of each species (*C. vaginalis* *n*=11; *C. delitrix* *n*=8; *H. mollis* *n*=10; *N. problematica* *n*=7; *T. californiana* *n*=8).

(Fig. 3B). Overall, both excurrent velocity (r_S=0.141, P<0.001) and oxygen removal (r_S=−0.221, P<0.0001) of *C. vaginalis* were not correlated with ambient current (Fig. 3A,B). The same is shown by the filtration to respiration (F/R) ratio, which did not change with increasing ambient flow, remaining at approximately 0.42± 0.03 l µmol^{-1} O_2 (r_S=0.232, P<0.0001, Fig. 3C).

For *C. delitrix*, excurrent velocity was positively correlated with ambient flow (r_S=0.485, P<0.0001; Fig. 4A,B); however, the osculum constricted in response to the flow generated by the pump, reducing in area from 4 cm^2 to less than 2 cm^2 (Fig. 4A). The reduced osculum size meant excurrent velocity increased but volumetric flow (volume filtered) decreased with more ambient

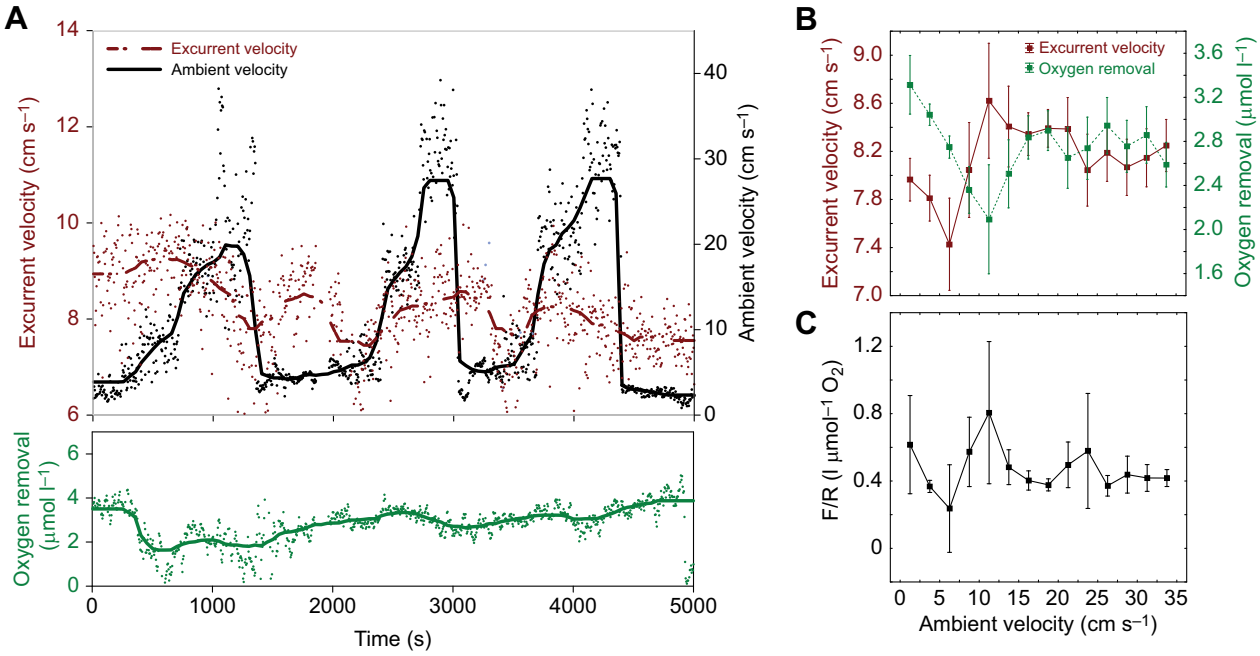

Fig. 3. Effect of ambient currents on excurrent velocity and oxygen removal in *Callyspongia vaginalis*. (A) Ambient (black) and excurrent (red) velocity (cm s^{-1}) recorded during an experiment in which ambient velocity was increased every 300 s (5 min) using an underwater aquarium pump over a single sponge. One experiment of three carried out is shown. The sponge responded to each change in ambient velocity, with a general trend of reducing excurrent velocity when ambient current was increased. Oxygen removal also slowly decreased over the course of the experiment. (B) Data in A plotted in bins of ambient flow (increments of 2.5 cm s^{-1}) show that excurrent velocity decreases in response to low ambient currents (0–5 cm s^{-1}) but increases in response to changes in ambient currents of 5–15 cm s^{-1}. Ambient currents greater than 15 cm s^{-1} cause no change in excurrent velocity. Changes in excurrent flow are followed by a change in oxygen removal, with a delay of ∼5 cm s^{-1}. There is no correlation between ambient and excurrent velocity (red; r_S=0.141, P<0.001) or between ambient velocity and oxygen removal (green; r_S=−0.221, P<0.0001). (C) The filtration to respiration (F/R) ratio did not change over the course of the experiment (r_S=0.232, P<0.0001).

Journal of Experimental Biology (2017) 220, 995-1007 doi:10.1242/jeb.146076

current (r_S=−0.407, P<0.0001; Fig. 4A,B). Oxygen removal (µmol h^{-1}) initially increased at ambient velocities of 0–5 cm s^{-1}, but overall oxygen removal was negatively correlated with ambient current (r_S=−0.456, P<0.0001; Fig. 4A,B). At ambient currents greater than 15 cm s^{-1} the excurrent velocity increased because of the constriction of the osculum, and oxygen removal decreased correspondingly. As with *C. vaginalis*, in *C. delitrix* there was no significant change in F/R ratio with increasing ambient flow (0.40 ±0.18 l µmol^{-1} O_2, r_S=0.307, P<0.0001; Fig. 4C).

Estimating the cost of filtration

Dimensions of each region of the aquiferous canal system for the five species of demosponges studied are given in Table 2. The path the water travels is illustrated in Fig. 5. Briefly, water flows in through minute holes (ostia) in the dermal membrane (a three-layered tissue) into a large subdermal space in four of the five species (except possibly for *C. delitrix*). From there, water enters into the largest incurrent canals, which branch into smaller and smaller canals leading to the choanocyte chambers (Fig. 6; Fig. S3). *Callyspongia vaginalis* is distinct from the other species in that the smallest incurrent canals empty into a common lacunar space that holds the choanocyte chambers as described by Johnston and Hildemann (1982) (Fig. 6A). Therefore, for *C. vaginalis*, openings between the choanocytes were considered the equivalent of prosopyles (Fig. 6B). In the other four species, water enters the choanocyte chambers from the smallest incurrent canal through one or more prosopyles. At the choanocyte chambers, water moves through the collar microvilli. In *H. mollis*, a set of cells forms a flat layer between all collars in the chamber (Fig. 6C). In both *N. problematica* and *C. vaginalis*, a dense mesh of glycocalyx occurs in the same region between each of the collars (Fig. 6B,D). Although a similar gasket has not yet been found in *T. californiana* and *C. delitrix* (Fig. 6E,F), this sort of structure may be more common in demosponges than has previously been appreciated because those made from mucus glycocalyx are difficult to preserve. A glycocalyx mesh was found between the microvilli of the choanocyte cells in each species studied (Fig. 6B), but in the case of *T. californiana* and *C. delitrix* it was only found in a few well-preserved choanocytes within a chamber. After passing through the glycocalyx mesh filter on the collar, the water flows into the chamber and from there out of the apopyle (exit of the sponge choanocyte chamber). In *T. californiana*, the apopyle consists of a sieve-plate (Fig. 6E); in other sponges, it is a circular aperture. From the apopyle, the water enters small excurrent canals that merge into increasingly larger canals before flowing out of the osculum.

Cross-sectional area, velocity of water and head loss for each region of the canal system calculated using the models of Riisgård and Larsen (1995) and Leys et al. (2011) are given in Table 3. In each species, the cross-sectional area increases as the water enters the choanocyte chambers (Table 3, Fig. 7). Velocity through each region (u_i) was calculated from total cross-sectional area of each region (i),

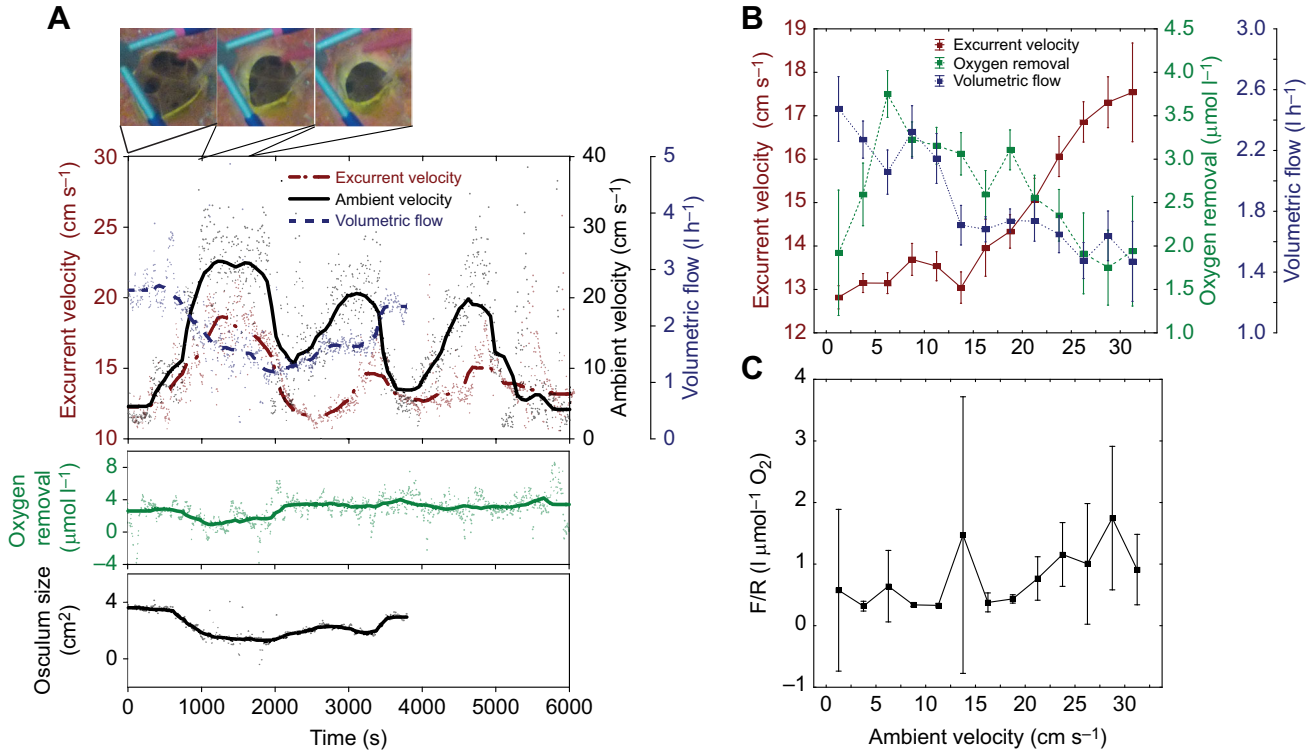

Fig. 4. Effect of ambient currents on excurrent flow rate and oxygen removal in *Cliona delitrix*. (A) Ambient velocity (black) was increased every 5 min using an underwater aquarium pump over a single sponge. One experiment of three carried out is shown. Excurrent velocity (red, dot-dashed line) increased with increasing ambient velocity, but contraction of the osculum (top images and lower graph) meant that the volume processed (blue, dashed line) decreased. Oxygen removal was variable over the course of the experiment. (B) Excurrent velocity binned by ambient flow (in 2.5 cm s^{-1} increments) shows that excurrent velocity increases when ambient flows are greater than 15 cm s^{-1}, and increased excurrent velocity is negatively correlated with oxygen removal. There is a positive correlation between ambient and excurrent velocity (red; r_S=0.485, P<0.0001), but a negative correlation between ambient velocity and volume filtered (blue; r_S=−0.407, P<0.0001). Because the osculum contracts, a smaller volume of water is processed, which also corresponds to a decrease in oxygen used (green; r_S=−0.456, P<0.0001). The initial increase in oxygen removal may be due to the energy required to contract the canals and osculum in response to the ambient current. (C) The F/R ratio did not change with different ambient current velocities (r_S=0.307, P<0.0001).

Journal of Experimental Biology

Table 2. Dimensions of the aquiferous canal system in sponges

	Haliclona permollis		*Aphrocallistes vastus*		*Neopetrosia problematica*		*Haliclona mollis*		*Tethya californiana*		*Callyspongia vaginalis*		*Cliona delitrix*	
Region of the aquiferous canal system	Diameter (μm)	Path length (μm)	Diameter (μm)	Path length (μm)	Diameter (μm)	Path length (μm)	Diameter (μm)	Path length (μm)	Diameter (μm)	Path length (μm)	Diameter (μm)	Path length (μm)	Diameter (μm)	Path length (μm)
Ostia	20.6		3.89	0.50	24.5	0.5	14.3	0.5	40.6	0.5	31.2	0.5	37.3	0.5
Subdermal space			90	82	242	86.1	95.0	50.6	177	105	168	131		
Large incurrent canal	50–340	3000	366	2000	383	2944	333	930	678	1118	407	923	294	1130
Medium incurrent canal				529	156	648	140	834	170	1118	195	725	144	969
Small incurrent canal				237	33	250	51.3	151.9	34.7	68.9	43.8	1	60.1	251
Prosopyles	1–5		2.15		3.60	0.5	2.37	0.5	4.52	0.5	1.61	0.5	2.59	0.5
Pre-collar space			2	2	1.3	2.6	5.7	3.6	1.6	2.2	0.5	2.6	0.69	2.19
Glycocalyx mesh			**0.045**	**0.010**	**0.095**		**0.166**		**0.059**		**0.052**		**0.118**	
Collar slit	**0.120**	**0.140**	**0.119**	**0.070**	**0.074**	**0.118**	**0.110**	**0.100**	**0.066**	**0.086**	**0.069**	**0.109**	**0.070**	**0.099**
Glycocalyx mesh			**0.045**	**0.010**										
Post-collar space			2	2	2.6	2.1	3.3	3.3	2.2	3.4	2.6	1.6	2.2	2.65
Chamber	30		56	56	23.3	23.3	28.5	28.5	21.1	21.1	19.7	19.7	16.0	16.0
Apopyle	14	1	26.4	2	16.0	0.5	14.1	0.5	0.90	0.5	5.97	0.5	4.23	0.5
Small excurrent canal				118	45.2	173	51.9	189	34.9	74	52.9	0.5	60.1	251
Medium excurrent canal					130	648	155	546	170	994	179	1096	144	969
Large excurrent canal	102–235	3000	405	2840	282	2944	411	930	678	994	339	1342	294	1130
Osculum	2300		44,734	279,000	3464	6676	5527	7420	8666	2184	16,209	198,410	22,666	9983
Chambers per mm^3	12,000		1876		9792		2684		14,403		14,358		35,175	
Collars per chamber	95		260		80		139		99		93		50	
Microvilli per collar	28		38		40		40		39		33		33	

Numbers represent means of three to 75 measurements taken from one to six images from either scanning electron microscopy (SEM) or histology and light micrographs. Dimensions of the collar slit, including the glycocalyx mesh on the collar, are in bold, representing the filtration apparatus. Data for *Haliclona permollis* are from Reiswig (1975a) and those for *Aphrocallistes vastus* are from Leys et al. (2011).

Journal of Experimental Biology (2017) 220, 995-1007 doi:10.1242/jeb.146076

Journal of Experimental Biology (2017) 220, 995-1007 doi:10.1242/jeb.146076

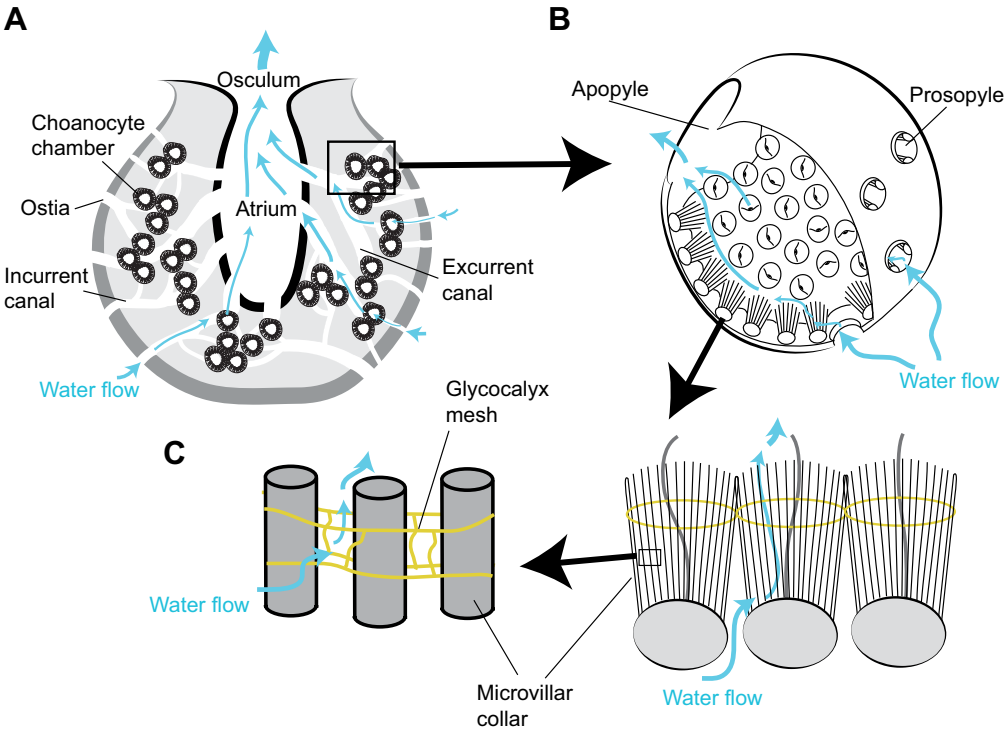

Fig. 5. Water flow through the aquiferous canal system of sponges. Schematic illustrating the path of water through the aquiferous system of sponges. (A) Water enters through pores (ostia) on the sponge surface, into incurrent canals to the choanocyte chambers, where the water is filtered, then out through the excurrent canals to the osculum. There is a huge increase in cross-sectional area of the aquiferous system as the water enters the choanocyte chambers, which slows the water for filtration. The cross-sectional area then decreases as the water leaves the choanocyte chambers, jetting the water out through the osculum. (B) Water enters the choanocyte chamber through prosopyles and exits via the apopyle. (C) Glycocalyx (yellow) forms a web that connects all of the collars of choanocyte cells together, such that water passes through the microvilli of the choanocyte chambers. Adjacent microvilli are also connected by a glycocalyx mesh (yellow).

A_i, and excurrent velocity out of the sponge osculum, u_{ex}, using Eqn 1. The effective velocity u_i through the collar slit of the two warm-water species *C. vaginalis* and *C. delitrix* was 0.018 and 0.017 mm s^{-1}, respectively, which is two to 10 times higher than the effective velocity in the temperate species (*N. problematica*=0.009 mm s^{-1}, *H. mollis*=0.006 mm s^{-1}, *T. californiana*=0.002 mm s^{-1}), a difference arising from the higher excurrent velocities of *C. delitrix* and *C. vaginalis*. The total head loss through the canal system – the sum of head loss through each region – is also five to 17 times higher for the tropical species (Table 3).

To determine the cost of filtration, the power required to pump water across the sponge, P_p, was calculated using the total head loss, ΔH, and volume flow rate, Q, and divided by the total measured oxygen removal, R_{tot} (Riisgård and Larsen, 1995), using the conversion 1 µl O_2 h^{-1}=5.333 µW (Riisgård, 1988) and the mean oxygen removal and volume flow rates reported in Table 1. Using the model by Riisgård and Larsen (1995), the estimates of the cost of filtration were quite variable, ranging from 1% for *T. californiana* to 15% for *C. delitrix*. The simplified model developed by Leys et al. (2011) gives the same relationship for cost of filtration between the five species of demosponge, although the range is slightly lower, from 1% for *T. californiana* and 12% for *C. delitrix*. Both models estimate a very similar cost of pumping for each species. Both of the warm-water species *C. vaginalis* and *C. delitrix* had the highest cost of pumping regardless of the model used (Table 3).

DISCUSSION

Our study aimed to assess the energetic cost of filtration in demosponges and to determine whether sponges reduce their cost of filtration by taking advantage of ambient currents. Of the five species of demosponges studied, the tropical species *C. delitrix* and *C. vaginalis* filtered the most water and extracted the most oxygen per gram of tissue. Because volumetric flow rate drives the model describing the energy required to overcome the resistance through the sponge aquiferous system, both tropical sponges have higher estimates of the cost of filtration than the three temperate demosponges *N. problematica*, *H. mollis* and *T. californiana*. Our data also show that the F/R ratio is constant for ambient flow velocity and therefore the cost of filtration depends only on the amount of water filtered. This suggests that the cost of filtration for demosponges varies by species and that reducing the volume of water filtered would reduce the cost of filtration in regions and seasons with lower food availability.

Interestingly, we found that demosponges can control the water flow through their bodies by responding behaviourally to changes in ambient flow. Both *C. delitrix* and *C. vaginalis* reduce the amount of water filtered at very high ambient velocities, which may be a mechanism to protect themselves from damage during storms. This reduction in the amount of water filtered at very high ambient velocities also suggests that neither species uses current-induced flow, despite the cost of filtration being higher than previously estimated.

The cost of pumping

Animals allocate energy to a variety of processes including growth, reproduction, feeding and digestion. For filter feeders, the energy allocated to feeding has been considered to be low, at 0.1–4% of total metabolism based on theoretical models (Jørgensen, 1955, 1986, 1988; Riisgård et al., 1993, 1988, 1989). In those studies, the cost of filtration was assumed to be equivalent to the energy lost owing to frictional resistance as water flows through the filter and canals. By changing filter size and volume flow rate using numbers gleaned from the literature, the estimate for the cost of filtration increased by up to five times previous estimates. This suggests that both filter dimensions and volume flow rates contribute substantially to the cost of pumping in filter-feeding invertebrates. It also suggests that accurate measurements of filter dimensions and volume flow rates are important when modelling the cost of filtration, and focused our attention on these for this study.

Although there were differences in gross morphology among the five species of sponge we studied, we found similar morphologies of the filter for each of the species studied. The cost of pumping was

Journal of Experimental Biology (2017) 220, 995-1007 doi:10.1242/jeb.146076

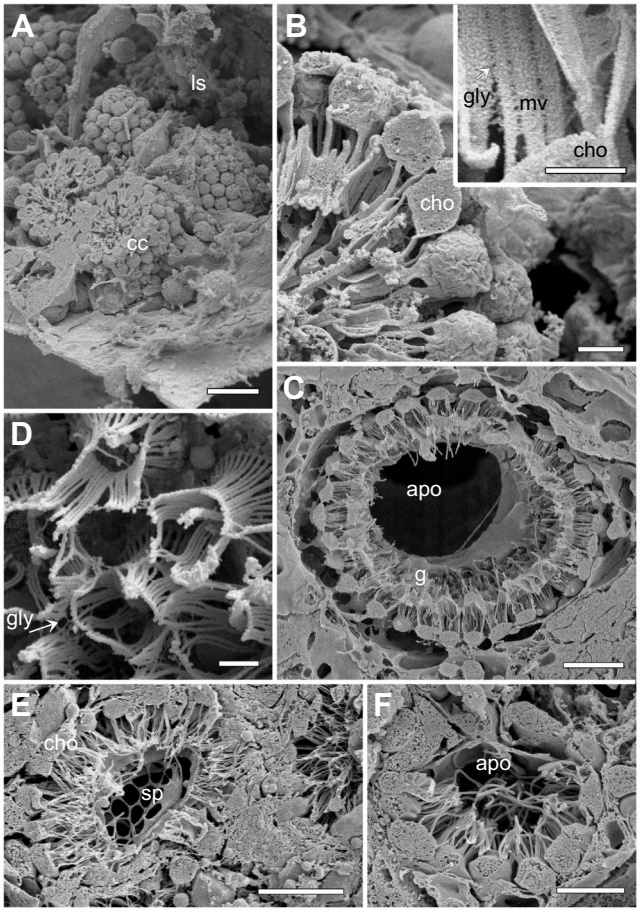

Fig. 6. Scanning electron micrographs of choanocyte chambers in five species of demosponges. (A,B) Choanocyte chambers (cc) of *Cliona vaginalis* within the lacunar spaces (ls). (B) Each choanocyte cell (cho) has a collar of microvilli (mv) that are connected by glycocalyx mesh (gly) (see inset). (C) Large choanocyte chamber in *Haliclona mollis* showing the cellular gasket (g) that connects each choanocyte cell. Water exits the chamber via the large apopyle (apo). (D) A glycocalyx mesh (gly) connects the collars in *Neopetrosia problematica*. (E) The apopyle in *Tethya californiana* consists of a sieve-plate (sp). (F) Smaller choanocyte chamber in *Cliona delitrix* with the flagella protruding from the apopyle. Scale bars: (A,C,E) 10 µm; (B) 2 µm, inset 1 µm; (D) 1 µm; (F) 5 µm.

variable, ranging from 1% (*T. californiana*) to 12–15% (*C. delitrix*) of the total oxygen consumed, assuming oxygen consumed is used for all metabolism including filtration. Previous estimates on the energetic cost of pumping in demosponges also show a large range, from 0.4% for *Haliclona urceolus* (Riisgård et al., 1993) to 25% for *Neogombata magnifica* (Hadas et al., 2008). Although this variability may reflect the use of theoretical models (Riisgård et al., 1993) compared with direct measurements (Hadas et al., 2008), our results suggest that the main variability in 'cost' arises from differences in the volume of water processed.

Whether a single equation was used for all structures of the aquiferous system (Leys et al., 2011) or different equations were used to describe potentially different aspects (aperture, duct, channel and lattice network openings) of the passages (Riisgård and Larsen, 1995), the estimate of cost was very similar. Small differences in cost found between the two models reflect differences in the dimensions and the velocity of water at the aperture or structure. The greatest head loss occurred at the glycocalyx mesh filter, which had the smallest dimensions and therefore offered the greatest resistance (Table 3). And yet while the mesh size was smaller in *T. californiana* than in *C. delitrix*, the head loss was far greater across the collar filter of *C. delitrix* because the velocity of water at its filter was substantially higher. Velocity at each aperture was governed by the exit velocity of each species, and so the two tropical species, having the largest volumetric flow rates (processing the most water), had the highest cost of filtration (Table 3). In addition, when individuals of each species filtered more water, they also consumed more oxygen (Fig. 2), demonstrating that the energetic cost of pumping depends on how much water is being pumped at any one time. This implies that sponges could save energy in times of low food availability by reducing the volume of water filtered.

That filtering more water costs more energy is not necessarily intuitive because sponges might use ambient flow to enhance the movement of water through their canal system. Our data demonstrate that neither *C. delitrix* nor *C. vaginalis* uses higher ambient flow to reduce the cost of filtration. Instead, both sponges actively modify their behaviour to increase or reduce the volume filtered. However, how a sponge changes its pumping rate and volume filtered is not known. One mechanism might be to increase the rate of flagellar beat in the choanocyte chambers or activate more pumping units. This would increase the velocity of water through the canal system and therefore increase the volume of water filtered. Dilation of the canals including the osculum diameter might also occur in addition to the increase in flagellar beat, which would increase the volume of water filtered. According to the Hagen–Poiseuille equation for flow through a pipe, the energy required to move water through a pipe is proportional to the square of the flow rate; therefore, an increase in water actively pumped through the canal system at any one time would increase the resistance and thus also the energetic cost of pumping. Similarly, because head loss is inversely proportional to the canal diameter to the power of four, constriction of the canals would result in a reduced volume flow rate, an increase in head loss, or a combination of both. Sponges likely control the rate of flagellar beating to save energy when the sponge contracts. We did not look at the energy spent on the flagellar beating nor the drag on the flagellum when estimating the cost of pumping, which is a limitation in the model and probably makes our estimates more conservative.

It is important to consider why the two tropical species of demosponge had higher volume flow rates and therefore higher estimates for the cost of filtration in this study. Differences in pumping rates between species can be caused by structural differences in the sponge canal system (Reiswig, 1975a), microbial content (Weisz et al., 2008) and tissue density (Turon et al., 1997). In addition, Riisgård et al. (1993) found that volume flow rate in *Haliclona urceolus* increased up to 10 times with a change in temperature from 6 to 15°C. The higher volume flow rate per gram weight in the two tropical species in this study therefore may be a result of the higher temperature of water and lower viscosity. However, because of the high energetic cost of filtering more water, it would only be adaptive to have such high volume flow rates if there is enough food available – either as picoplankton to be filtered from the water or from endosymbionts – to support the high energetic needs. We did not measure carbon flux in these species but this is a planned next step.

Sponges are found in almost every marine and freshwater habitat and, with the exception of carnivorous sponges, all feed on ultraplankton and dissolved organic carbon. Increasing cross-sectional area through the canal system slows the velocity of water, enabling food capture either in the small incurrent canals or at the filter. Slight differences in filtration ability and size of

Table 3. Morphometric model of the aquiferous system in five species of demosponges

	Neopetrosia problematica				*Haliclona mollis*				*Tethya californiana*				*Callyspongia vaginalis*				*Cliona delitrix*			
			H (μm H_20)				*H* (μm H_20)				*H* (μm H_20)				*H* (μm H_20)				*H* (μm H_20)	
Region of the aquiferous canal system	A_i (mm^2)	u_i (mm s^{-1})	Riisgård and Larson (1995)	Leys et al. (2011)	A_i (mm^2)	u_i (mm s^{-1})	Riisgård and Larson (1995)	Leys et al. (2011)	A_i (mm^2)	u_i (mm s^{-1})	Riisgård and Larson (1995)	Leys et al. (2011)	A_i (mm^2)	u_i (mm s^{-1})	Riisgård and Larson (1995)	Leys et al. (2011)	A_i (mm^2)	u_i (mm s^{-1})	Riisgård and Larson (1995)	Leys et al. (2011)
Ostia	3.37	1.04	111	4	0.90	3.90	709	42	1.38	1.76	113	2	12.8	0.68	51	1	2.82	6.57	409	9
Subdermal space	19.7	0.18	56	7	22.2	0.16	239	96	16.7	0.14	46	26	21.8	0.40	10	12				
Large incurrent canal	15.9	0.22	16	16	14.4	0.24	6	6	21.7	0.11	2	2	14.1	0.62	9	9	3.31	5.60	338	338
Medium incurrent canal	7.21	0.49	26	26	3.21	1.09	45	45	24.8	0.10	19	19	2.70	3.25	47	47	2.57	7.22	1026	1026
Small incurrent canal	5.79	0.61	491	491	4.16	0.84	278	278	3.66	0.66	25	25	3.67	2.39	3	3	1.71	10.84	1969	1969
Prosopyles	494	0.007	438	103	346	0.010	922	330	172	0.014	380	71	55.2	0.159	3434	1806	17.7	1.04	9714	3186
Pre-collar space	255	0.014	49	49	775	0.005	5	5	504	0.005	55	55	170	0.051	6768	6768	264	0.070	19,158	19,158
Collar slit	**376**	**0.009**	**288**	**797**	**546**	**0.006**	**471**	**73**	**1237**	**0.0020**	**147**	**521**	**492**	**0.018**	**668**	**8202**	**1095**	**0.017**	**2300**	**1969**
Post-collar space	412	0.009	13	13	405	0.009	9	9	1077	0.0022	6	6	566	0.015	17	17	1019	0.018	37	37
Chamber	408	0.009	2	2	171	0.020	1	1	488	0.005	0	0	406	0.022	3	3	674	0.027	4	4
Apopyle	208	0.02	1	0	44.6	0.08	4	0	110	0.02	14	13	40.3	0.22	8	1	52.1	0.36	15	3
Small excurrent canal	4.66	0.75	6	6	6.79	0.52	24	24	2.47	0.98	6	6	0.52	16.9	0	0	1.71	10.84	97	97
Medium excurrent canal	3.47	1.01	128	128	6.33	0.55	52	52	24.8	0.10	149	149	2.87	3.05	2288	2288	2.57	7.22	1985	1985
Large excurrent canal	1.21	2.90	165	165	13.1	0.27	13	13	21.7	0.11	1	1	3.04	2.88	140	140	3.31	5.60	371	371
Osculum	0.26	13.66	10	33	0.12	30.44	47	33	0.11	21.95	25	3	0.15	59.33	179	176	0.17	110.41	622	8
Volume flow rate, Q (ml min^{-1})			9.0				48.6				82.1				742				2668	
Respiration, R_{tot} (μW)			87				790				1396				14,218				42,102	
Head loss, ΔH (μm H_20)			2138	2303			1881	1008			826	771			4066	6185			14,307	11,304
Pumping power, P_p (μW)			3	3			15	8			11	11			504	766			6377	5038
Cost of pumping, η (%)			3.70	3.99			1.89	1.01			0.80	0.74			3.54	5.38			15.15	11.97

A_i is the estimated total cross-sectional area for each region from the dimensions listed in Table 2. The velocity of water flow through each area u_i was calculated from cross-sectional area A_i and measured excurrent velocity u_{ex} out of the osculum using Eqn 1. Head loss H in each region was calculated using Eqns A1–A5 from dimensions and velocity u_i of each region. Riisgård and Larson's (1995) model used a different equation of head loss for each region of the aquiferous canal system, whereas Leys et al.'s (2011) model used only Eqn A2. The sum of the head loss ΔH and measured volume flow rate are used to calculated the pumping power P_p using Eqn A6. The cost of pumping η (%) is then estimated using Eqn A7 from the pumping power P_p and the measured respiration rate R_{tot}. The collar slit is in bold, representing the filtration apparatus.

Journal of Experimental Biology (2017) 220, 995-1007 doi:10.1242/jeb.146076

Journal of Experimental Biology (2017) 220, 995-1007 doi:10.1242/jeb.146076

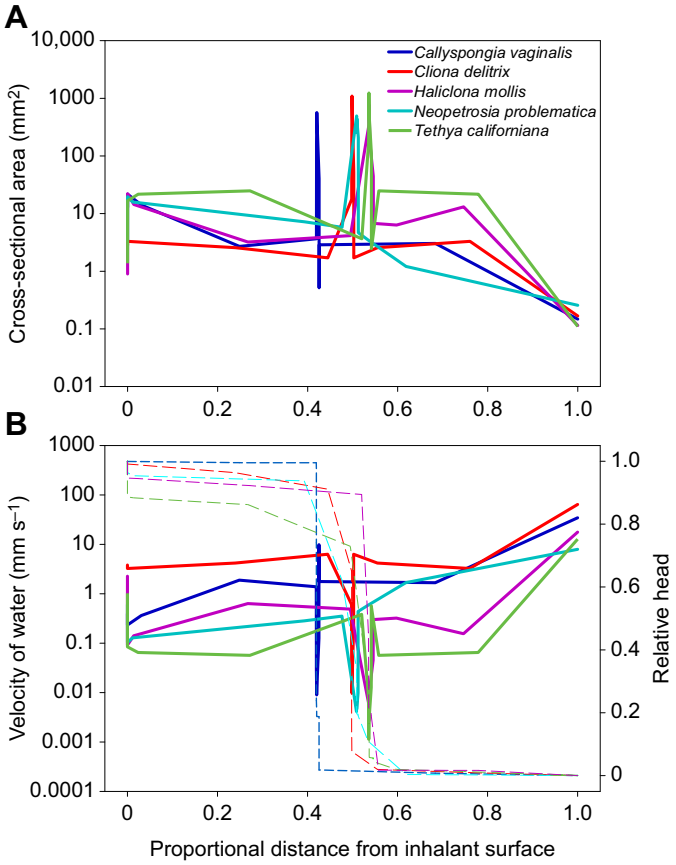

Fig. 7. Morphometric model for five species of demosponges. (A) Total cross-sectional area of the aquiferous canal systems (from Table 2) from the inhalant surface to the osculum for five species of demosponges: *H. mollis* (purple), *N. problematica* (cyan), *T. californiana* (green), *C. vaginalis* (blue) and *C. delitrix* (red). (B) Estimated water velocity (solid lines) and relative head loss (dotted lines) through the aquiferous canal system, from Table 3, as water travels from the inhalant surface to the osculum for the same five species of demosponges.

plankton captured between different species of sponges are known (Reiswig, 1975b; Turon et al., 1997; Yahel et al., 2007). There is little information, however, on the relationship between filtration ability, diet and microarchitecture of the aquiferous canal system. Among the five species studied here, slight variations in the architecture of the aquiferous canal system were found, such as the lacunar space in *C. vaginalis* and the sieve-plate apopyle of *T. californiana.* We also found wide differences in the velocities of water measured out of the osculum, but similar velocities of water at the filter (Table 3). This suggests that despite wide differences in volume flow rates and adaptations to a variety of habitats and ecological niches, the canal system of sponges is designed to slow the velocity of water down to a certain speed that enables food capture at the filter. The small differences that were found in both velocities at the filter and filter dimensions may reflect small differences in preferred plankton size or filtration ability. A smaller mesh size may allow the sponge to capture smaller food particles but, because of the higher cost of filtration, may also restrict the volume of water processed. Our model predicted that both tropical species *C. vaginalis* and *C. delitrix* had faster velocities of water at the collar filter. *Callyspongia vaginalis* lacks the small incurrent canals leading into the choanocyte chambers, suggesting that it does not rely on pinacocyte capture of plankton in the canals.

Ambient currents do not enhance excurrent velocity

One way to reduce the cost of pumping in sponges would be to take advantage of ambient currents by using passive flow. In both *C. delitrix* and *C. vaginalis*, excurrent volume flow rates were not correlated to the ambient currents, suggesting that these species do not use passive flow. Rather, both species decreased their volume flow rate when ambient velocities reached a certain level, which may be to reduce damage caused by high currents or resuspension of sediments during storms (Gerrodette and Flechsig, 1979; Tompkins-MacDonald and Leys, 2008; Bannister et al., 2012).

We suggest that the discrepancy in our results and those of Vogel, who first described the apparent use of induced current by sponges (Vogel, 1974, 1977), are due to his use of excurrent velocity rather than volume flow rate and the use of individual points in time rather than a full time series. The increased excurrent velocity recorded by Vogel (1977) in the species *Amphimedon viridis* (referred to as *Haliclona viridis*), *Ircinia variabilis* (referred to as *Ircinia fasciculata*) and *Aplysina fistularis* (referred to as *Verongia fistularis*) may have been behavioural responses, as shown here in *C. delitrix* in which contraction of the osculum caused increased excurrent (exit) velocity, but reduced volumetric flow rate as ambient currents increased. A full time series with measurements of the osculum diameter throughout would indicate whether Vogel's findings were actually a result of current-induced flow or rather a behavioural response to the increased current.

Other sponges have also been reported to show reduced excurrent flow with increased ambient flow. Savarese et al. (1997) noted that two individuals of the globose freshwater sponge *Baikalospongia bacillifera* in Lake Baikal monitored over a diel cycle showed negative correlations between ambient and excurrent flow rates. In addition, they noted periodic cessation of pumping on the order of minutes to hours that did not correlate with ambient flow. Reiswig (1971) also found periodic oscular closures and therefore cessations of pumping in *Tethya crypta* that were negatively correlated to wave action. Here, we found that both *C. vaginalis* and *C. delitrix* reduced the volume of water filtered when ambient currents reached a certain threshold. Therefore, some demosponges show a large amount of control of filtration despite fluctuations in the ambient water velocity.

General conclusions

The over-arching finding of this work is that the energetic costs of sponge pumping are closely coupled to volumetric flow (how much water is filtered). We found a considerable variation in flow rates and corresponding costs, with tropical sponges having higher volumetric flow rates and costs. The difference may be related to food availability and temperature. We also found that despite the variation in costs, the similarity in architecture and design of the aquiferous canal system is such that the velocity of water slows at the filter, although each species accomplishes this in slightly different ways, thus making them all well suited to feed on ultraplankton and dissolved organic carbon.

For the three temperate demosponges, our estimates for the cost of pumping are comparable to those found by Riisgård et al. (1993) for what he termed the 'standard sponge'. However, the two tropical demosponges we studied had much higher volume flow rates with a much higher cost of pumping: the cost of pumping for *C. delitrix* was more comparable to the cost of pumping for other sponges found by both Leys et al. (2011) and Hadas et al. (2008). It is likely that the habitat and ecological niche of sponges have led to adaptations in body form and physiology over time, and together

these play a large role in differences in cost of pumping. Our third main finding was that despite the higher costs for the two tropical sponges, ambient flow is not a positive driver of flow through the sponge and is therefore not used to reduce the cost of filtration. Instead, both of these sponges responded to increased ambient currents by reducing the volume filtered. In the shallow sandy habitat of both *C. delitrix* and *C. vaginalis*, increased ambient flow results in resuspension of particles. Demosponges have sensory cilia in their osculum, which allow them to sense and respond to changes in their environment (Ludeman et al., 2014). Reiswig (1975a) showed that several species of tropical demosponge responded to storm events by reducing filtration, and so it is likely that the demosponges we studied here respond to changes in ambient currents to reduce damage to their filter that would be caused by intake of sediments resuspended during high ambient currents.

APPENDIX

Equations used to calculate resistance through the canal system

Following the approach by Riisgård and colleagues (Jørgensen et al., 1986; 1988; Riisgård, 1988; 1989; Riisgård et al., 1993; Riisgård and Larsen, 1995), the hydraulic head loss through each region of the canal system H_i may be due to apertures, frictional resistance in canals, or pressure drop across lattice nets. Most flows in biological systems occur at low Reynolds numbers $Re=ud/\nu$, where d is the diameter of tube or aperture, u is mean velocity and ν is kinematic viscosity. As water flows from a large diameter canal into a smaller one, the flow becomes fully developed after a length of approximately $L_d \approx 0.1dRe$. Flow in the sponge canals is at low Re and is fully developed. Head loss for ostia, prosopyles and apopyles was calculated using eqn 15 from Riisgård and Larsen (1995) for creeping flow through a circular aperture with diameter d (equation originally from Happel and Brenner, 1983):

$$\Delta H_i = 6\pi\nu u_{i-l}/gd, \tag{A1}$$

where u_{i-l} is mean velocity of the flow upstream of the structure and $\boldsymbol{g}$ is the acceleration of gravity. Head loss at the canals was calculated using a rendition of the Hagen–Poiseuille equation for fully developed laminar flow in a circular tube of length L and radius r, which is eqn 19 in Riisgård and Larsen (1995) (originally in Fox et al., 1998):

$$\Delta H_i = 8\nu u_{i-l}L/gr^2. \tag{A2}$$

For the subdermal space, which is a region below the dermal membrane, head loss was calculated using eqn 21 in Riisgård and Larsen (1995) for flow between parallel plates spaced l distance apart (originally in Walshaw and Jobson, 1962):

$$\Delta H_i = 12\nu u_{i-l}L/gl^2, \tag{A3}$$

where L is the length of the subdermal space and l is the width of the subdermal space. Head loss across the rectangular lattice mesh, eqn 17 in Riisgård and Larsen (1995) and originally described by Silvester (1983), is calculated as:

$$\Delta H = K\nu u_{i-l}/gh, \tag{A4}$$

where $K = 8\pi/(1-2ln\left(\frac{\pi d}{h_0}\right)+\left(\frac{\pi d}{h_0}\right)^2/6)$; $h_0 = h_1h_2/\sqrt{(h_1^2+h_2^2)}$; d is the diameter of the cylindrical fiber; and h represents the dimensions of the mesh where: $h = \frac{h_1h_2}{h_1+h_2}$, h_1 is the width of the mesh and h_2 is the length of the mesh. The contribution of head loss from the velocity of water leaving the sponge osculum can be estimated from the kinetic head loss, eqn 22 in Riisgård and Larsen (1995), as:

$$\Delta H_i = u_{ex}^2/2g, \tag{A5}$$

where u_{ex} is the velocity of water leaving the osculum. The total head loss through the system is equal to the sum of the head losses at each region of the canal system.

As a comparison to the model by Riisgård and Larsen (1995), we also used the simplified model developed by Leys et al. (2011) which assumes head loss through each region of the aquiferous canal system can be calculated based on the Hagen–Poiseuille equation for fully developed laminar flow in a tube (Eqn A2).

As the values used for both the density of seawater, ρ, and kinematic viscosity, ν, depend on the temperature of seawater, a temperature of 12°C was used for the temperate demosponges and a temperature of 30°C was used for the tropical demosponges. To estimate the overall pump efficiency (η), and therefore the cost of pumping, we used eqn 25 from Riisgård and Larsen (1995):

$$\eta = \frac{P_p}{R_{tot}}, \tag{A6}$$

where R_{tot} is the total metabolic power expenditure (total measured respiration) and P_p is the pumping power expressed by the linear energy equation for steady, incompressible flow through a controlled volume, eqn 24 in Riisgård and Larsen (1995):

$$\rho g\Delta HQ = P_p. \tag{A7}$$

Here, Q is the volume flow rate through the system and ΔH is the total pressure drop, or head loss, through the system.

Acknowledgements

We thank the directors and staff at the Bamfield Marine Sciences Center, Bamfield, British Columbia, and the Smithsonian Tropical Research Station, Bocas del Toro, Panama, for use of facilities; N. Lauzon and N. Trieu for assistance with field work and histology, respectively; and A. Kahn and G. Yahel for valuable comments on an earlier version.

Competing interests

The authors declare no competing or financial interests.

Author contributions

D.A.L., S.P.L. and M.A.R. conceived the experiments; S.P.L. collected the sponges; D.A.L., S.P.L. and M.A.R. performed the experiments; D.A.L. carried out the electron microscopy, histology, statistical analysis and morphometric modelling; D.A.L. and S.P.L. wrote the paper.

Funding

D.A.L. acknowledges a Nortek student equipment grant for use of a Vectrino Profiler for portions of this work, and the Company of Biologists for a Travelling Fellowship to carry out the work in Panama. Funding for this work came from the Natural Sciences and Engineering Research Council of Canada (NSERC) through a Discovery Grant to S.P.L. and a National Science Foundation (NSF) CAREER Grant (NSF-OCE 1151314) to M.A.R.

Data availability

Data for this study are accessible at the University of Alberta Education Resource Archive (ERA): https://doi.org/10.7939/R36688W8N and https://doi.org/10.7939/R39Z90Q23.

Supplementary information

Supplementary information available online at http://jeb.biologists.org/lookup/doi/10.1242/jeb.146076.supplemental

References

Bannister, R. J., Battershill, C. N. and de Nys, R. (2012). Suspended sediment grain size and mineralogy across the continental shelf of the Great Barrier Reef: impacts on the physiology of a coral reef sponge. *Cont. Shelf Res.* **32**, 86-95.

Journal of Experimental Biology

Best, B. (1988). Passive suspension feeding in a sea pen: effects of ambient flow on volume flow rate and filtering efficiency. *Biol. Bull.* **175**, 332-342.
Bidder, G. P. (1923). The relation of the form of a sponge to its currents. *Q. J. Microsc. Sci.* **67**, 293-323.
Denny, M. (1993). *Air and Water: The Biology and Physics of Life's Media*. Princeton, NJ: Princeton University Press.
Diaz, M. C. (2005). Common sponges from shallow marine habitats from Bocas del Toro Region, Panama. *Carib. J. Sci.* **41**, 465-475.
Fox, R. W., McDonald, A. T. and Pritchard, P. J. (1998). *Introduction to Fluid Mechanics*, Vol. 5. New York: John Wiley & Sons.
Genin, A., Karp, L. and Miroz, A. (1994). Effects of flow on competitive superiority in scleractinian corals. *Limnol. Oceanogr.* **39**, 913-924.
Gerrodette, T. and Flechsig, A. O. (1979). Sediment-induced reduction in the pumping rate of the tropical sponge *Verongia lacunosa*. *Mar. Biol.* **55**, 103-110.
Gili, J.-M. and Coma, R. (1998). Benthic suspension feeders: their paramount role in littoral marine food webs. *Trends Ecol. Evol.* **13**, 316-321.
Griffiths, C. L. and King, J. A. (1979). Energy expended on growth and gonad output in the ribbed mussel *Aulacomya ater*. *Mar. Biol.* **53**, 217-222.
Hadas, E., Ilan, M. and Shpigel, M. (2008). Oxygen consumption by a coral reef sponge. *J. Exp. Biol.* **211**, 2185-2190.
Happel, J. and Brenner, H. (1983). *Low Reynolds Number Hydrodynamics: with Special Applications to Particulate Media.* The Hague: Springer-Verlag.
Harris, P. and Shaw, G. (1984). Intermediate filaments, microtubules and microfilaments in epidermis of sea urchin tube foot. *Cell Tissue Res.* **236**, 27-33.
Johnston, I. S. and Hildemann, W. H. (1982). Cellular organization in the marine demosponge *Callyspongia diffusa*. *Mar. Biol.* **67**, 1-7.
Jørgensen, C. (1955). Quantitative aspects of filter feeding in invertebrates. *Biol. Rev.* **30**, 391-453.
Jørgensen, C. (1975). Comparative physiology of suspension feeding. *Annu. Rev. Physiol.* **37**, 57-79.
Jørgensen, C. B. (1966). *Biology of Suspension Feeding*. London: Pergamon Press.
Jørgensen, C. B., Famme, O., Kristensen, H. S., Larsen, P. S., Møhlenberg, F. and Riisgård, H. U. (1986). The bivalve pump. *Mar. Ecol. Prog. Ser.* **34**, 69-77.
Jørgensen, C. B., Larsen, P. S., Møhlenberg, F. and Riisgård, H. U. (1988). The mussel pump: properties and modeling. *Mar. Ecol. Prog. Ser.* **45**, 205-216.
Knott, N. A., Davis, A. R. and Buttemer, W. A. (2004). Passive flow through an unstalked intertidal ascidian: orientation and morphology enhance suspension feeding in *Pyura stolonifera*. *Biol. Bull.* **207**, 217-224.
LaBarbera, M. (1977). 1. Theory, laboratory behavior, and field orientations. *Paleobiology* **3**, 270-287.
Leys, S., Yahel, G., Reidenbach, M., Tunnicliffe, V., Shavit, U. and Reiswig, H. (2011). The sponge pump: the role of current induced flow in the design of the sponge body plan. *PLoS ONE* **6**, e27787.
Ludeman, D., Farrar, N., Riesgo, A., Paps, J. and Leys, S. (2014). Evolutionary origins of sensation in metazoans: functional evidence for a new sensory organ in sponges. *BMC Evol. Biol.* **14**, 3.
Murdock, G. R. and Vogel, S. (1978). Hydrodynamic induction of water flow through a keyhole limpet (Gastropoda, Fissurellidae). *Comp. Biochem. Physiol. A Physiol.* **61**, 227-231.
Newell, R. C. and Branch, G. M. (1980). The influence of temperature on the maintenance of metabolic energy balance in marine invertebrates. *Adv. Mar. Biol.* **17**, 329-396.
Reiswig, H. M. (1971). *In situ* pumping activities of tropical Demospongiae. *Mar. Biol.* **9**, 38-50.
Reiswig, H. M. (1975a). The aquiferous systems of three marine Demospongiae. *J. Morphol.* **145**, 493-502.
Reiswig, H. M. (1975b). Bacteria as food for temperate-water marine sponges. *Can. J. Zool.* **53**, 582-589.
Riisgård, H. U. (1988). The ascidian pump: properties and energy cost. *Mar. Ecol. Prog. Ser.* **47**, 129-134.
Riisgård, H. U. (1989). Properties and energy cost of the muscular piston pump in the suspension feeding polychaete *Chaetopterus variopedatus*. *Mar. Ecol. Prog. Ser.* **56**, 157-168.
Riisgård, H. and Larsen, P. (1995). Filter-feeding in marine macro-invertebrates: pump characteristics, modelling and energy cost. *Biol. Rev.* **70**, 67-106.
Riisgård, H. U. and Larsen, P. S. (2001). Minireview: ciliary filter feeding and bio-fluid mechanics – present understanding and unsolved problems. *Limnol. Oceanogr.* **46**, 882-891.
Riisgård, H., Thomassen, S., Jakobsen, H., Weeks, J. and Larsen, P. (1993). Suspension feeding in marine sponges *Halichondria panicea* and *Haliclona urceolus*: effects of temperature on filtration rate and energy cost of pumping. *Mar. Ecol. Prog. Ser.* **96**, 177-188.
Savarese, M., Patterson, M. R., Chernykh, V. I. and Fialkov, V. A. (1997). Trophic effects of sponge feeding within Lake Baikal's littoral zone. 1. In situ pumping rates. *Limnol. Oceanogr.* **42**, 171-178.
Shiino, Y. (2010). Passive feeding in spiriferide brachiopods: an experimental approach using models of Devonian *Paraspirifer* and *Cyrtospirifer*. *Lethaia* **43**, 223-231.
Silvester, N. R. (1983). Some hydrodynamic aspects of filter feeding with rectangular-mesh nets. *J. Theor. Biol.* **103**, 265-186.
Thompson, R. J. and Bayne, B. L. (1972). Active metabolism associated with feeding in the mussel *Mytilus edulis* L. *J. Exp. Mar. Biol. Ecol.* **9**, 111-124.
Tompkins-MacDonald, G. J. and Leys, S. P. (2008). Glass sponges arrest pumping in response to sediment: implications for the physiology of the hexactinellid conduction system. *Mar. Biol.* **154**, 973-984.
Trager, G. C., Hwang, J.-S. and Strickler, J. R. (1990). Barnacle suspension-feeding in variable flow. *Mar. Biol.* **105**, 117-127.
Turon, X., Galera, J. and Uriz, M. J. (1997). Clearance rates and aquiferous systems in two sponges with contrasting life-history strategies. *J. Exp. Zool.* **278**, 22-36.
Vogel, S. (1974). Current-induced flow through the sponge, *Halichondria*. *Biol. Bull.* **147**, 443-456.
Vogel, S. (1977). Current-induced flow through living sponges in nature. *Proc. Natl. Acad. Sci. USA* **74**, 2069-2071.
von Dassow, M. (2005). Flow and conduit formation in the external fluid-transport system of a suspension feeder. *J. Exp. Biol.* **208**, 2931-2938.
Walshaw, A. C. and Jobson, D. A. (1962). *Mechanics of Fluids*. London: Longman.
Weisz, J., Lindquist, N. and Martens, C. (2008). Do associated microbial abundances impact marine demosponge pumping rates and tissue densities? *Oecologia* **155**, 367-376.
Yahel, G., Marie, D. and Genin, A. (2005). InEx – a direct *in situ* method to measure filtration rates, nutrition, and metabolism of active suspension feeders. *Limnol. Oceanogr. Methods* **3**, 46-58.
Yahel, G., Whitney, F., Reiswig, H. M., Eerkes-Medrano, D. I. and Leys, S. P. (2007). In situ feeding and metabolism of glass sponges (Hexactinellida, Porifera) studied in a deep temperate fjord with a remotely operated submersible. *Limnol. Oceanogr.* **52**, 428-440.
Young, C. and Braithwaite, L. (1980). Orientation and current-induced flow in the stalked ascidian *Styela montereyensis*. *Biol. Bull.* **159**, 428-440.